Regular Article

PHAGOCYTES, GRANULOCYTES, AND MYELOPOIESIS

Transcriptome analysis highlights the conserved difference between embryonic and postnatal-derived alveolar macrophages

Sophie L. Gibbings,[1] Rajni Goyal,[1] A. Nicole Desch,[2] Sonia M. Leach,[3] Miglena Prabagar,[1] Shaikh M. Atif,[1] Donna L. Bratton,[1] William Janssen,[4] and Claudia V. Jakubzick[1,2]

[1]Department of Pediatrics, [2]Department of Immunology and Microbiology, [3]Integrated Center for Genes, Environment, and Health, and [4]Department of Medicine, National Jewish Health and University of Colorado Denver Anschutz Campus, Denver, CO

Key Points

- Of the 30 000 genes, there are ~0.1% genes whose expression is linked to the origin of the cell rather than the environment.
- *Marco* was most conserved by embryonic origin and not altered by the environment, whereas *C1qb* and *Plbd1* were most conserved by adult origin.

Alveolar macrophages (AMs) reside on the luminal surfaces of the airways and alveoli where they maintain host defense and promote alveolar homeostasis by ingesting inhaled particulates and regulating inflammatory responses. Recent studies have demonstrated that AMs populate the lungs during embryogenesis and self-renew throughout life with minimal replacement by circulating monocytes, except under extreme conditions of depletion or radiation injury. Here we demonstrate that on a global scale, environment appears to dictate AM development and function. Indeed, transcriptome analysis of embryonic host-derived and postnatal donor-derived AMs coexisting within the same mouse demonstrated >98% correlation and overall functional analyses were similar. However, we also identified several genes whose expression was dictated by origin rather than environment. The most differentially expressed gene not altered by environment was *Marco*, a gene recently demonstrated to have enhancer activity in embryonic-derived but not postnatal-derived tissue macrophages. Overall, we show that under homeostatic conditions, the environment largely dictates the programming and function of AMs, whereas the expression of a small number of genes remains linked to the origin of the cell. (*Blood*. 2015;126(11):1357-1366)

Introduction

Alveolar macrophages (AMs) reside on the luminal surfaces of the airways and airspaces where they serve critical roles in host defense and alveolar homeostasis, ingesting particulates and microbes that are constantly encountered in the lungs. Importantly, under most circumstances the phagocytosis of inhaled foreign agents is silent, such that inflammatory responses are activated only under circumstances when host defenses become overwhelmed.[1] Indeed, compared with macrophages from other sites, AMs are relatively ineffective at initiating immune responses.[2,3] Furthermore, compared with other tissue macrophages, they display a unique repertoire of cell surface molecules and have a distinct transcriptome profile.[4-6]

AMs are now known to derive primarily from fetal liver monocytes and self-renew throughout life with minimal replenishment from circulating monocytes.[7-15] This self-renewal is not only maintained under steady-state conditions, but also during acute and chronic inflammation.[16] These concepts were illustrated in lung-protected bone marrow (BM) chimera studies in which lead shields were used to protect AMs during radiation. Eight weeks after BM transplantation, the lungs of these chimeras contained AMs of host origin, whereas circulating monocytes were donor-derived.[16] In these chimeric mice, we showed that during inflammation (lipopolysaccharide or influenza A infection), BM donor-derived monocytes were rapidly recruited into

the airspaces. However, once inflammation resolved, the remaining AMs were still predominantly of the host origin, suggesting that under most circumstances postnatal monocytes do not give rise to AMs.[16] The self-renewal and maintenance of host-derived AMs has also been illustrated in parabiotic mouse studies, which demonstrated that AMs are minimally replenished by postnatal circulating monocytes.[10,11]

Overall these studies demonstrate that in both perturbed and unperturbed lungs, there is minimal replacement of self-renewing embryonic-derived AMs by postnatal monocytes. However, under circumstances in which substantial loss of embryonic-derived AMs is induced, replacement by postnatal monocytes can occur (as observed for embryonic-derived Langerhans cells and Kupffer cells[17,18]), for example by intratracheal delivery of diphtheria toxin to CD11c-diphtheria toxin receptor mice,[19] intratracheal delivery of clodronate-loaded liposomes (CLLs),[20-22] and full-body exposure to high-dose irradiation.[23] Similarly, humans that undergo allogeneic BM transplantation after myeloablative-conditioning regimens have mixed AM chimerism.[24,25]

A key question that arises from each of these settings is whether AMs with different ontogeny (ie, embryonic-derived vs postnatal-derived monocytes) exhibit similar or differential phenotypes and functions, and whether the environment of the pulmonary airspaces is dominant in

determining their programming state. To address this, we created a mouse model to identify differences in the transcriptomes of embryonic (host) vs postnatal (donor)-derived AMs in the same mouse where embryonic-derived AMs normally self-renew, but in inadvertent circumstances may be replaced by postnatal BM-derived monocytes that subsequently mature into tissue macrophages. Accordingly, chimeric mice were created in which both the host and donor-derived AMs coexist within the lungs of the same mouse. This provided an unbiased analysis of the transcriptional, phenotypic, and functional capabilities of AMs that derive from host vs donor origins.

Materials and methods

Mice

CD45.1 and CD45.2 C57BL/6, p40-YFP BL/6, and UBC-GFP BL/6 mice were purchased from Jackson Laboratories. Mice were used for experiments at 6 to 8 weeks of age, housed in a specific pathogen-free environment at National Jewish Health, and used in accordance with protocols approved by the Institutional Animal Care and Utilization Committee.

Development of host and donor-derived AMs within the same mouse

To achieve a relatively equal proportion of host and donor-derived AMs within the same mouse, we followed a method previously used by Janssen et al.[16,26] Recipient mice, either CD45.1 or CD45.2 C57BL/6, were anesthetized with 1X Avertin and positioned between lead strips 1-cm thick by 2-cm wide to protect the lungs from radiation. Radiation was provided at 900 rads. Six hours after irradiation, recipient mice received BM cells either CD45.2 or CD45.1 C57BL/6. Eight weeks post-BM transplantation, host AMs were depleted using 50 μL of CLLs. Eight weeks post-CLL treatment in BM-chimeric mice, the mice were sacrificed to sort host and donor-derived AMs.

Flow cytometry

Bronchoalveolar lavage (BAL) was obtained by flushing the airways four times with 1 mL of phosphate-buffered saline (PBS) containing 0.5 mM EDTA and 0.1% bovine serum albumin. BAL fluid was resuspended in fluorescence-activated cell sorter (FACS) blocking solution and stained for 30 minutes with conjugated Abs. The following purified monoclonal antibodies were used for staining: fluorescein isothiocyanate (FITC)–conjugated anti-F4/80 (Serotech); PE-conjugated anti–Siglec-F; PerCP Cy5.5-conjugated to anti-Ly6C; PB-conjugated monoclonal antibodies anti-CD11b or CD11c; allophycocyanin (APC)–conjugated to CD64, CD45.2, Siglec-F; PE-Cy7–conjugated to CD45.1 or CD11c; V500-conjugated to CD45.2 or MHCII; and APC-Cy7-conjugated to CD45.2 (monoclonal antibodies were purchased from eBioscience, BD Biosciences, or BioLegend). Biotin-conjugated to polyclonal MerTk was purchased from R&D Systems. Appropriate isotype-matched controls were obtained from eBioscience, BD Biosciences, or BioLegend. AM counts were performed as previously shown.[20] We measured total AM counts by the complete acquisition of cells collected and present within an FACS tube via flow cytometry. Flow cytometry was performed using the LSR II (BD Biosciences), and data were analyzed with FlowJo (Tree Star).

AM isolation and sorting strategy for microarray analysis

Microarray analysis from chimeric mice. Whole mouse gene arrays were performed using Affymetrix Mouse Gene 2.0 ST v1 microarray. PBS–perfused lungs were minced and digested using 400 μg/mL Liberase (Roche) for 25 minutes, and then filtered twice through a 100-μm nylon strainer. Single cell suspension was enriched using anti-CD11c conjugated Miltenyl beads. Enriched cells were stained with Pacific Blue-conjugated anti-B220, anti-CD3, anti-NK1.1, anti-CD103, anti-CD11b, and anti-Gr1, along with 4,6 diamidino-2-phenylindole to use as a dump channel, doublet cells were excluded and

Pacific Orange conjugated anti-MHC II was also used to dump MHC II–expressing cells. CD11c$^+$SiglecF$^+$ AMs were identified with APC Cy7-conjugated anti-CD11c (N418 clone), PE-conjugated anti-Siglec F (BD Biosciences). Donor and host-derived AMs were identified with PECy7-conjugated CD45.1 and APC-conjugated CD45.2 (eBioscience) and sorted using a BD Aria Fusion. Antibodies and controls were purchased from BD Biosciences or eBioscience. Isolation of AMs was performed for set 1 and set 2: sorting strategy shown in supplemental Figure 1. Set 1, donor-derived AMs expressed CD45.2 and host-derived AMs expressed CD45.1. set 2, donor-derived AMs expressed CD45.1 and host-derived AMs expressed CD45.2. Host and donor-derived AMs were pooled from four mice per sort. Only one sort was performed per day providing two samples: host and donor-derived AMs. A total of eight sorts were performed: four sorts for set 1 (CD45.2 donor into CD45.1 hosts) and four sorts for set 2 (CD45.1 donor into CD45.2 hosts). RNA was extracted using TRIzol reagent according to the manufacturer's instructions (Invitrogen Life Technologies) followed by RNA clean-up using RNAeasy Mini kit (Qiagen). RNA obtained was subjected to microarray analysis using an ABI instrument.

Microarray analysis for alveolar and interstitial macrophages from naïve mice. RNA was amplified and hybridized on the Affymetrix Mouse Gene 2.0 ST microarray. Raw data were normalized using the robust multiarray algorithm and a common threshold for positive expression at 95% confidence across the dataset was determined to be 120. Differentially expressed probe sets between populations were selected using a Student t test with Bonferroni correction ($P < .05$ and twofold change). Signature transcripts were visualized using the "Heat Map Viewer" module of GenePattern (http://www.broadinstitute.org/cancer/software/genepattern/) and pathway enrichment and in signatures was interrogated using List2Network software (http://amp.pharm.mssm.edu/lachmann/upload/register.php). Principal component analysis was conducted using MATLAB by using robust multiarray average (RMA) normalized and log2 transformed expression levels as previously described.[27] All datasets have been deposited at National Center for Biotechnology Information/Gene Expression Omnibus under accession number GSE15907.

Intranasal deliveries of phagocytic targets

Administration of intranasal deliveries was performed using an optimized delivery system.[28] Mice were completely anesthetized with 1X Avertin: *tert*-amyl alcohol content at 2.5% and 2,2,2 tribromoethanol (T1420; TCI America) at a concentration of 50 mg/kg. FITC-labeled apoptotic cells, *Escherichia coli* bioparticles, *Staphylococcus aureus* bioparticles, or Zymosan A bioparticles or yellow-green 2 μm carboxylated beads (Molecular Probes) were diluted in PBS. A 50 μL solution was delivered via the intranasal route with a final concentration of 20×10^6 apoptotic cells, 4 μg bioparticles, and 30×10^6 carboxylated beads (Molecular Probes). Phagocytosis by AMs was assessed 2 hours postdelivery of phagocytic targets. Five minutes before flow cytometry analysis, quenching was performed by adding 50 μL of trypan blue into a 300 μL volume of BAL cells.

Apoptotic cell preparation

Single-cell suspension of thymocytes was obtained by mashing the thymus through a 40 μm nylon filter. Thymocytes were labeled with a final concentration of 10 μM CFSE (Invitrogen) for 10 minutes at 37°C. Postlabeling, thymocytes were incubated in 30 mL of RPMI 1640 containing 10% fetal calf serum followed by 2-hour incubation at 37°C to remove free carboxyfluorescein diacetate succinimidyl ester. After 2 hours of incubation, thymocytes were exposed to 60 mJ UV radiation (StrataLinker 1800; AgilentTechnologies) to induce apoptosis. Apoptotic cell were washed twice in RPMI 1640 prior to instillation.

Intracellular cytokine staining

Bronchoaveolar lavage was performed 4 hours after intranasal delivery of FITC-conjugated E. coli bioparticles along with 10 μg/mL Brefeldin A. After lavage, AMs were surface stained in the presence of 10 μg/mL Brefeldin A. After surface staining, cells were fixed and permeabilized using the Foxp3 permeabilization kit provided by eBioscience. Cells were stained with PerCP Cy5.5 conjugated tumor necrosis factor (TNF)-α and APC conjugated IL-1β or isotype control (BD Biosciences).

Quantitative reverse-transcription–PCR

RNA purified from sorted cells was reverse transcribed into complementary DNA using oligo(dT)$_{12-18}$ primer (Invitrogen Life Technologies). Primers for polymerase chain reaction (PCR) analysis were Actin sense, GAAATCGTGCGTGACATCAAAG and antisense, TGTAGTTTCA TGGATGCCACAG; Marco sense, GAAACAAAGGGGACATGGG and antisense, TTCACACCTGCAATCCCTG; Sema3e sense, CGCGATCA CTACAAGCAAAA and antisense, AGCCAATCAGCTGCAAGAAT; Wfdc10 sense, TCCAGGAATCTGCTGCTCTT and antisense, GTCTT GGTGGGCTTCACAAT; Plbd1 sense, CAAAACATCAAAGCGCAGAA and antisense, CCAACTTGAGTGGGCAAAAT; Ifi205 sense, TCCACA ACCCAGGAAGAGAC and antisense, GGGCTCTGAGTGGAGAACAG; Wwtr1 sense, AACAGTAGCTCAGATCCTTTCCTCTA and antisense, CCGC TCTGCCTCATCACTTGGTC. Primers were purchased from Gene Link and used according to their recommendations.

Microscopy of murine lungs

BM chimeras: host p40-YFP BL/6 (AMs do not express YFP) and donor UBC-GFP BL/6. Eight weeks post-BM transplantation host AMs were depleted using 50 μL of CLLs. Eight weeks post-CLL treatment in BM-chimeric mice lungs were perfused with 4% paraformaldehyde containing 20% sucrose in PBS and then inflated with 1 mL of optimum cutting temperature (O.C.T.) compound (Tissue-Tek). Finally, the lungs were excised and embedded in O.C.T. and stored at −80°C. Then 10 μM sections were cut and blocked with 1% bovine serum albumin and stained with anti-SiglecF antibody (BD Biosciences) for 30 minutes. After three washes with PBS, the section was incubated with anti-rat Cy3 (Jackson ImmunoResearch) for 30 minutes. Samples were mounted using fluorescent mounting medium containing 4′,6 diamidino-2-phenylindole (DAPI; Vecta-Shield). Images were obtained using an AxioVision microscope Carl Zeiss.

Statistics on host- and donor-derived AMs

Array analysis. Affymetrix Mouse Gene 2.0 ST v1 microarray data were processed to obtain log$_2$ expression Signal values using Affymetrix Power Tools (apt) software suite to perform RMA with background correction, quantile normalization, and median polish summarization. Probes were annotated using the file MoGene-2_0-st-v1.na34.mm10.transcript.csv provided by Affymetrix. Nonexpressed and invariant transcripts (26 929 of 41 345 probes) were removed using a median variance filter while enforcing a Benjamini-Hochberg false discovery rate of 0.1.[29] A further 6950 probes with no gene annotation were removed. The final data set of log$_2$ RMA expression values for 7566 probes (8263 unique genes) was visualized and analyzed using packages and custom scripts within the R statistical software (v3.1.1) (http://www.r-project.org/). Heatmaps were created using the pheatmap_0.7.7 package, with row scaling for expression profiles (http://CRAN.r-project.org/package=pheatmap). Differential analysis was performed with limma_3.22.1 using a classic sum-to-zero parameterization without an interaction term (Y ∼ strain + treatment).[30,31] Probes were considered differentially expressed if the Benjamini-Hochberg adjusted P value (ie, q value) was ≤0.05 for either the strain effect (CD45.1 vs CD45.2, 118 probes) or the treatment effect (host vs donor, 305 probes). Fold changes in set 1 or set 2 were calculated as the mean replicate expression level in host-derived AM divided by the mean replicate expression level in donor-derived AM.

Scatter plot statistical analysis was conducted using InStat and Prism software (GraphPad Software). All results were expressed as the mean ± standard error of the mean. Statistical tests were performed using 2-tailed Student t test. A value of P < .05 was considered statistically significant.

Results

Model for the coexistence of host- and donor-derived AMs

To assess the transcriptome differences dictated by origin instead of environment, we created a mouse model where both host and donor-derived AMs coexist. First, wild-type mice (either CD45.1 or CD45.2)

were exposed to γ irradiation while lead strips shielded their lungs to protect host-derived AMs. After irradiation, congenic BM cells that expressed the alternate CD45 antigen were adoptively transferred via intravenous injection to replenish the BM (Figure 1A).[26] Eight weeks post BM-reconstitution, >98% of AMs were of the host origin (day 0; Figure 1B), whereas circulating monocytes were >99% donor-derived (supplemental Figure 2A). To create an environment in which host- and donor-derived AMs coexist, BM-reconstituted mice were given CLLs via the intranasal route. Intranasal delivery of CLLs depletes AMs ~80% to 85% by day 2 (Figure 1C).[20,22] Lack of inflammation within the airways and full recovery of AM numbers was observed by day 35 (supplemental Figure 2B-C), at which point AMs within the lungs of the same mouse were ~50% host-derived and ~50% donor-derived (Figure 1B-C). Morphologic assessment of host- and donor-derived AMs were similar (Figure 1D).

Importantly, we created congenic BM chimeras in both directions. Thus in "set 1," CD45.2 BM was transplanted into CD45.1 hosts to create animals in which donor-derived AMs expressed CD45.2 and host-derived AMs expressed CD45.1. In "set 2," the reciprocal transplant was performed (CD45.1 BM into CD45.2 hosts). The rationale for creating reciprocal chimeric sets arises from the fact that CD45.1 expressing cells appear to have a slight developmental advantage over those that express CD45.2. For instance, in a BM chimeric model in which an equal ratio of CD45.1 and CD45.2 donor cells were adoptively transferred, circulating monocytes derived slightly more from CD45.1 compared with CD45.2.[32,33] Furthermore in noninflamed parabiotic mice, although there is minimal replacement of the native AM from donor-derived monocytes, a few CD45.1 monocytes appear to more readily seed the AM population compared with CD45.2.[11] Therefore, creating reciprocal sets of chimeras allowed us to specifically analyze differences between the host- and donor-derived AMs and to eliminate potentially confounding differences that arise from the congenic markers, CD45.1 and CD45.2.

AMs from reciprocal BM chimeras were isolated 8 weeks after clodronate-loaded liposome treatment, and host vs donor-derived AMs were sorted for transcriptome analysis. One sort was performed each day from either set 1 or set 2, which yielded both host- and donor-derived AMs. A total of eight sorts were performed resulting in 16 samples. Replicates of four for CD45.1 host-derived AMs, CD45.2 host-derived AMs, CD45.1 donor-derived AMs, and CD45.2 donor-derived AMs were analyzed for their gene transcription using Affymetrix microarrays (Figure 2A).

Gene array of host- and donor-derived AMs are tightly correlated

The first step was to assess the similarity (or difference) between the donor and host-derived AMs by correlation plots. As a control to establish the strength of correlation between donor and host-derived AMs, replicates from a murine endothelial cell line, Bend3, were also analyzed. The Pearson correlation plots revealed that genes from donor- and host-derived AMs were tightly correlated (99%-97%). This strength of correlation was similar to those observed for endothelial cell line replicates (99%-100%). In comparison, correlation values for AMs vs endothelial cells ranged from 84% to 85% (Figure 2A).

To validate the microarrays, protein expression of several well-accepted AM markers was assessed at the transcriptional level (Figure 2B).[4,5,34] Similar protein and mRNA expression was observed between host- and donor-derived AMs for CD11c, CD64, and MerTk. In contrast, F4/80 only at the gene level displayed slightly less expression in donor-derived AMs compared with host-derived AMs, whereas Siglec-F displayed less protein and messenger RNA expression
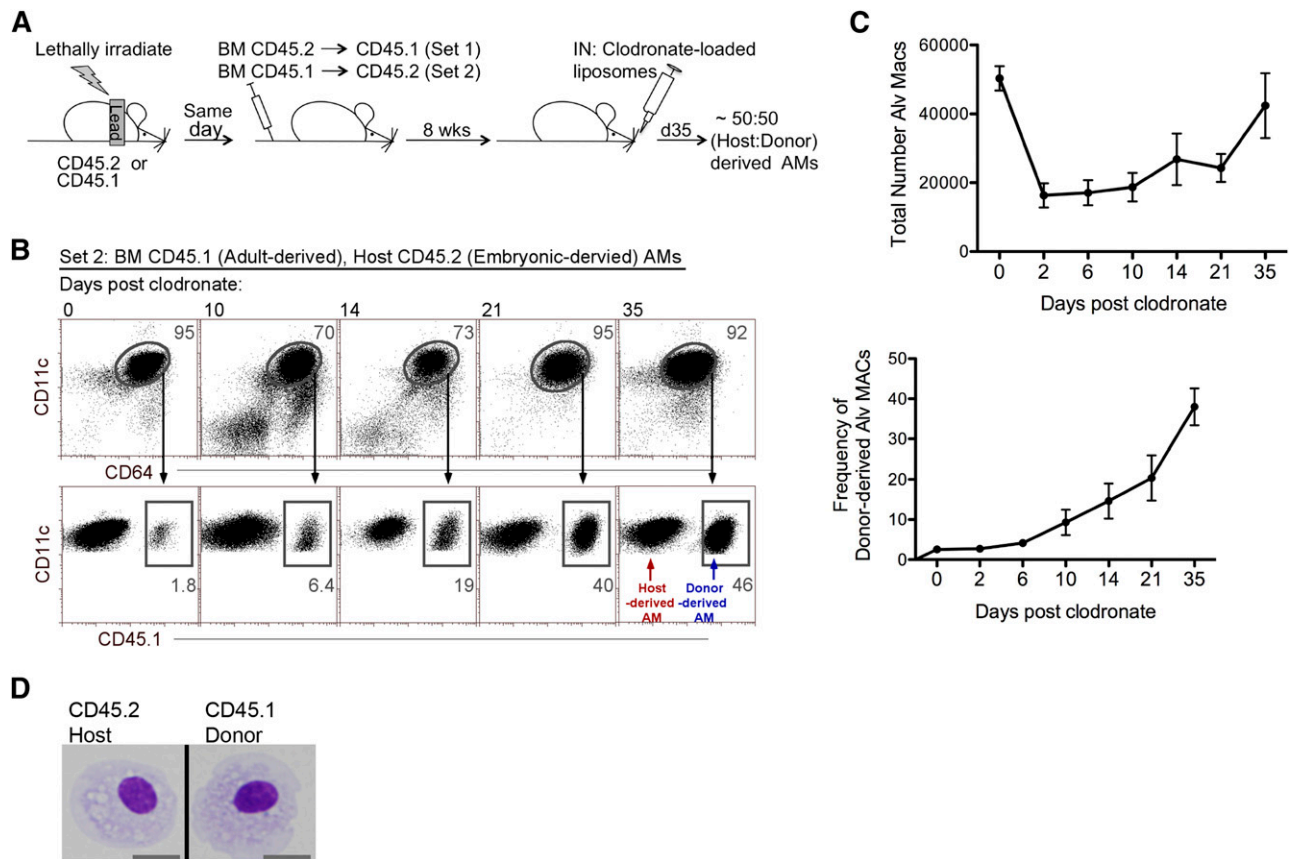
Figure 1. Model for the coexistence of host- and donor-derived AMs. (A) Strategy: First, lungs of mice were protected with lead prior to irradiation. Postirradiation, congenic BM cells were transferred intravenously. Set 1: irradiated CD45.1 mice received CD45.2 BM. Set 2: irradiated CD45.2 mice received CD45.1 BM. Eight weeks later, mice were treated with CLL via intranasal (IN) delivery to deplete AMs. By day 35, post-CLL treatment, mice contained ~50% host- or donor-derived AMs. (B) Time course analysis of the reconstitution of host- and donor-derived AMs post-CLL treatment. Frequency of contribution of CD45.1$^+$ donor-derived CD11c$^+$CD64$^+$ AMs was analyzed (illustrated by set 2). Data represents 3 independent experiments. (C) Time course analysis of the total numbers of AM post-CLL treatment. Data represents 3 independent experiments. (D) Morphologic analysis of BM reconstituted mice at day 35 post-CLL. Cytospin of sorted host- and donor-derived AM. MACs, macrophages.

in donor-derived AMs compared with host-derived AMs (supplemental Figure 1 and Figure 2B). Although the magnitude of the Siglec-F changes was small (half-log less protein expression by FACS analysis for donor-derived AM and 1.4-fold gene difference for host- vs donor-derived AM), the difference was statistically significant. Siglec-F is a member of the sialic acid–binding immunoglobulin-type lectin family of inhibitory immunoreceptors (Siglecs), and while its precise function on AMs is unknown, it has been suggested to inhibit cell activation via cytosolic immunoreceptor tyrosine-based inhibitory motif domains.[35] Finally, we confirmed that genes selectively expressed on monocytes, neutrophils, T cells, and B cells were not expressed on the AM micro-arrays (supplemental Figure 3 and Figure 2B). These data demonstrate that known cell surface proteins expressed on AMs are also expressed at the gene level, validating our arrays.

In a recent study, it was shown that 21 transcription factors were selectively expressed by AMs compared with other tissue macrophages.[5] In our current study, 20 of these transcription factors were found to display identical gene expression levels between host- and donor-derived AMs (Figure 2C). The one exception was the transcription factor Wwtr1,[36] known to regulate cellular growth, which was more highly expressed in the host-derived AM. Taken as a whole, these data demonstrate striking similarities in global gene expression between host- and donor-derived AMs. Furthermore, the alignment of AM specific transcription factors from donor-derived AMs compared with host-derived AMs suggests that environment dictates the overall outcome of a precursor cell with the exception of a few genes.

Gene expression differences between host- and donor-derived AMs

Although the majority of expressed genes appeared to be responsive to the local environment, we then focused on those that were differentially expressed between host- and donor-derived AMs. Using a four-way scatter plot, we examined genes with probes on the microarray that were significantly differentially expressed (false discovery rate = 0.05) and had a greater than 2-fold difference in expression between host- and donor-derived AMs in both reciprocal chimera sets. As shown in Figures 3A-B, 24 genes were more highly expressed in host-derived AMs, whereas 11 genes were more highly expressed in donor-derived AMs. An additional 7 genes were differentially expressed in CD45.1 vs CD45.2 AMs, an effect that was independent of origin.

Of the 24 genes that were more highly expressed in host-derived AMs, *Marco* exhibited the greatest fold difference (13.8 for set 1 vs 11.3 for set 2). Furthermore, we randomly selected and confirmed by quantitative PCR 4 genes expressed higher for host-derived AM and 2 for donor-derived AMs (Figure 3C). Interestingly, *Marco* was recently demonstrated to have enhancer activity in embryonic-derived, but not postnatal-derived tissue macrophages.[37] Therefore, although environment shapes the overall gene expression outcome of a macrophage precursor cell, *Marco* is clearly an exception because donor-derived AMs do not express *Marco* compared with host-derived AMs (Figure 3A-C). Marco is a class A scavenger receptor that serves as a pattern-recognition receptor for bacteria and is involved in host
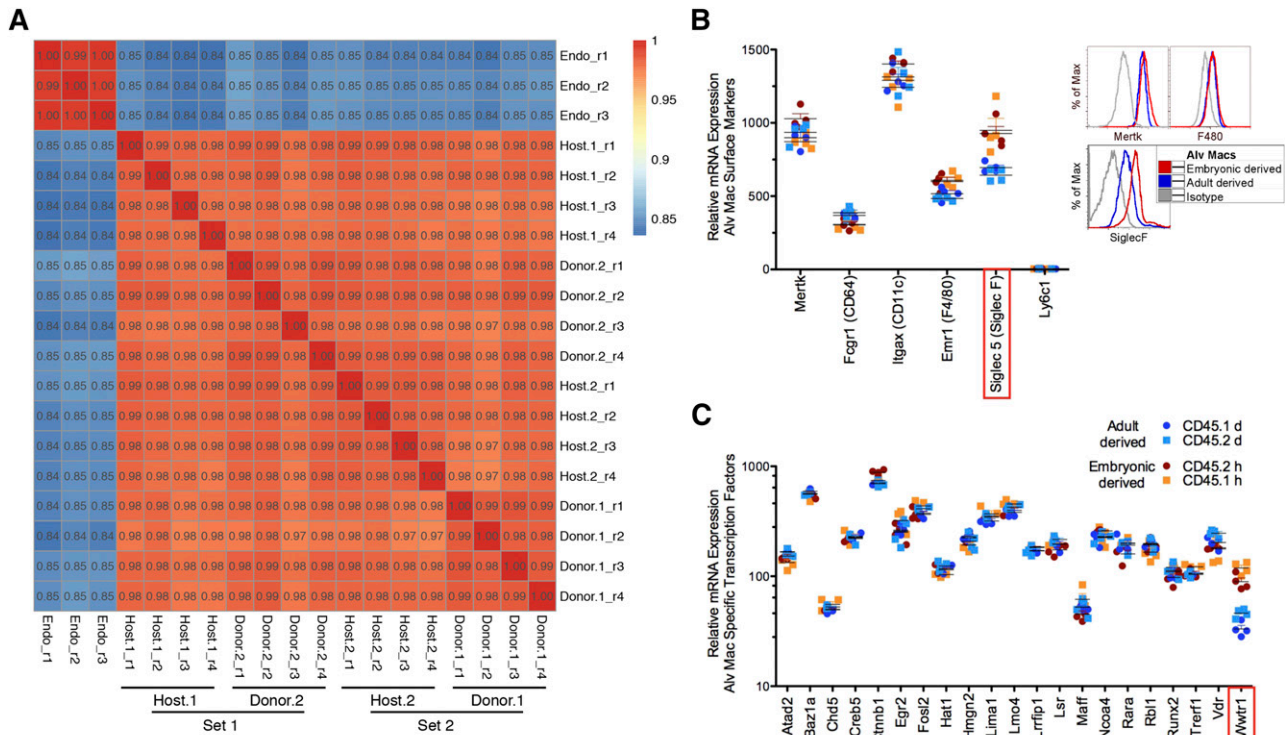
Figure 2. Transcriptional profiles of host- and donor-derived AMs. For microarray analysis, AMs of host and donor origin were fluorescence-activated cell sorted from whole lung digests from lead shielded BM reconstituted mice 8-weeks post-CLL delivery. (A) Pearson correlation plots comparing host- and donor-derived AMs from either CD45.1 (host.1 and donor.1) or CD45.2 (host.2 and donor.2). Data demonstrates experimental sets containing 4 replicates (r) of each sample type. An endothelial cell line (Bend3) was used as a control for correlation comparison (Endo). (B) Messenger RNA (mRNA) microarray expression for surface molecules on host-derived AMs (red, CD45.2 host; orange, CD45.1 host) and donor-derived AMs (blue, CD45.1 donor; light blue, CD45.2 donor) (left). Protein expression by flow cytometry for Siglec F, MertK, and F4/80 on host- and donor-derived AMs (right). Protein data represents 8 independent experiments. (C) The mRNA microarray expression levels of lung specific transcription factors. Statistically significant differences (Student t test; $P < .05$) between host- and donor-derived AMs are highlighted in red box. Alv Macs, alveolar macrophages.

defense.[38-40] Intriguingly, when the functions of the remaining genes were annotated, 3 additional genes with putative roles in the recognition and removal of microbial pathogens were identified: *Colec12, cdc42bpa,* and *Wfdc10. Colec12* encodes for scavenger receptor C-type lectin and has been implicated in recognition and phagocytosis of fungi and bacteria,[41,42] whereas cdc42 is required for cytoskeletal rearrangement during phagocytosis.[43] *Wfdc10* encodes for domains present in serine proteinase inhibitors that may inhibit the proteolytic activity of microbial proteases. The remaining genes are thought to play roles in development, cell differentiation, and proliferation, (*Sema3e, Wwtr1, Bmpr1, Mustn, Meis1, Prickle2, Rasef*), signal transduction (*Lphn3, Lrig3*), and metabolism (*Igf2bp2, Lepr*). Six genes are unclassified (RIKEN complementary DNA clones and FlyBase gene models, referred to as Rik and Gm genes, respectively) and 2 (*Fam115a, Fam135a*) represent genes of unknown function.

Eleven genes were more highly expressed in donor-derived AMs. Of these, 3 also have potential roles in host defense and inflammation, including *C1qb, Pyhin1,* and *Slamf7. C1qb* encodes for the β chain of C1q, the first component of the classical complement pathway, whereas PYHIN1 (pyrin and HIN domain family member 1) functions as a microbial DNA sensor and induces interferon-β and nitric oxide production in macrophages.[44,45] Conversely, SLAMF7, a member of the signaling lymphocyte activation molecule family may dampen inflammatory responses in mononuclear phagocytes.[46] Finally, 4 of the genes may promote cell proliferation and survival (*Apbb2, Mef2c, Akt3, Ifi205*).

Overall, these data demonstrate that of approximately 30 000 genes present on the microarrays, only a small fraction of these genes

(<0.1%) displayed a twofold or greater difference between host- and donor-derived AMs. If reciprocal BM transplantation with CD45.1 and CD45.2 congenic mice were not performed, an additional 7 genes could have been mistakenly identified as differentially expressed by host- or donor-derived AMs. For example, 6 genes were expressed at greater levels for CD45.1 compared with CD45.2-derived AMs (Figure 3A). Of the ones with known function (*N*-acetylneuraminate pyruvate lyase (*Npl*) and glutamate-ammonia ligase (*Glul*) regulate production of glutamine and pyruvate for cellular energy, and perhaps explain the slight developmental advantage observed for CD45.1 over CD45.2 cells in mixed BM chimera mice and parabiosis.[11,32,33] We only observed 1 gene in favor of CD45.2 compared with CD45.1, SHC SH2 domain-binding protein 1-like protein (*Shcbp1l*). Finally, we also examined genes with fold changes in the same direction that were a twofold change in one set and slightly below a twofold change for the other set (supplemental Figures 4 and 5). Accordingly, the noted differences observed for CD45.1 and CD45.2 gene expression illustrate the value of performing bidirectional studies with reciprocal chimeras.

Similar phagocytic uptake and proinflammatory cytokine production by host- and donor-derived AMs

Although few gene differences were observed between host- and donor-derived AMs, 2 phagocytic scavenger receptors were differentially expressed (Figure 3A). A hallmark feature of macrophages is their phagocytic capacity. Therefore, next we investigated whether the phagocytic processes themselves differed between the host- and
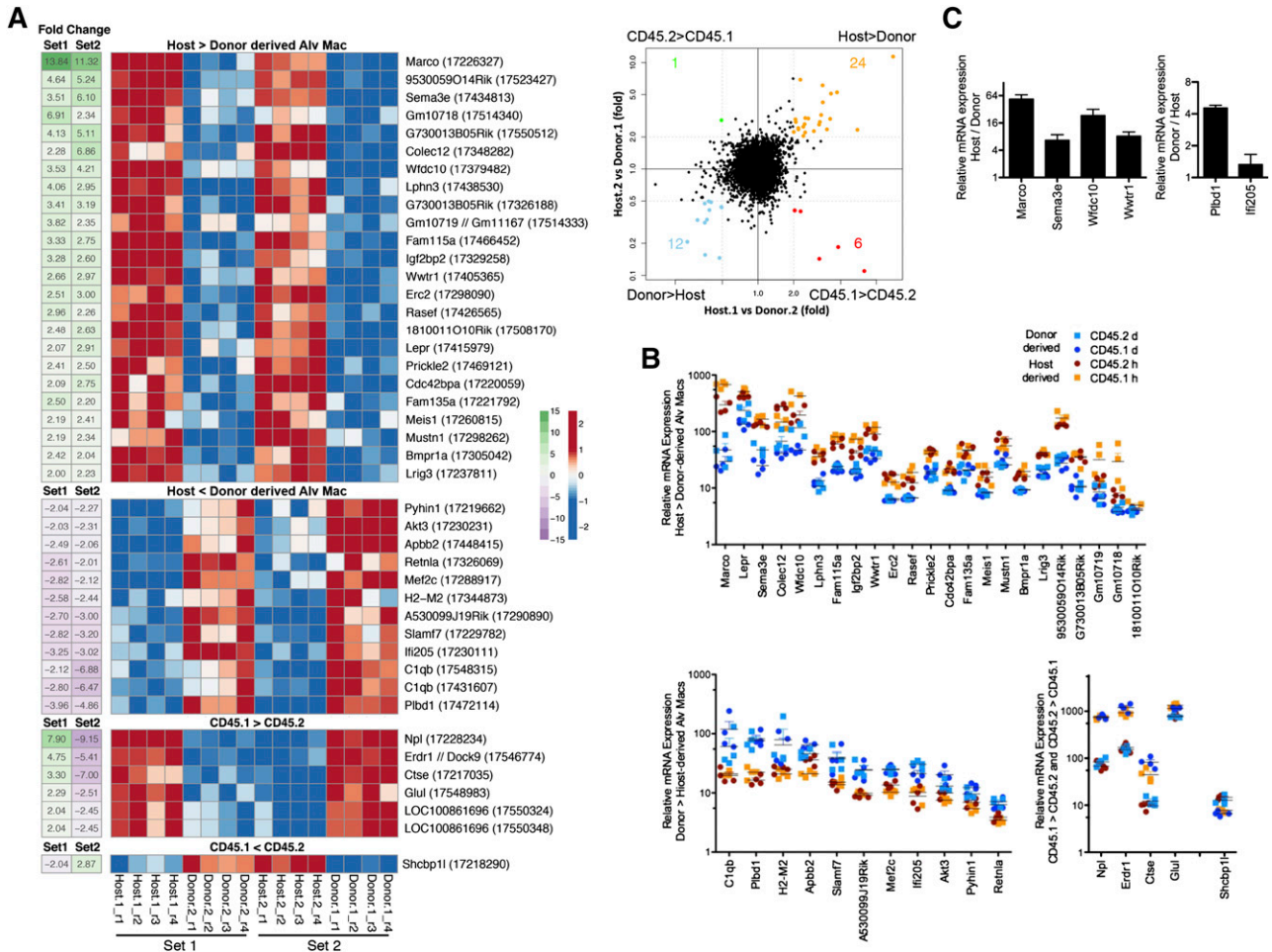
Figure 3. Differences in gene expression between host- and donor-derived AMs. (A) Heatmap illustrating expression level profiles for gene with a significant (limma, false discovery rate = 0.05) difference for host vs donor-derived AM or CD45.1 vs CD45.2-derived AM) and at least a twofold change difference between host- and donor-derived AMs in both set 1 (host.1 vs donor.2) and set 2 (host.2 vs donor.1) (left). Probe identifiers are shown in parentheses after gene symbols annotating each row. Row-scaled expression levels shown using red-blue scale, fold-change shown using green-purple scale. Right, four-way scatter plot comparing fold change in set 1 and fold change in set 2. Genes highlighted in orange, blue, red, or green represent the 4 possible extreme groups host > donor, host < donor, CD45.1 > CD45.2, and CD45.1 < CD45.2, respectively, whose data were shown in the heatmap (left). Gray dashed lines depict a twofold change difference. (B) Scatter plot of relative expression of messenger RNA (mRNA) for genes represented on heat map. (C) Confirmation of Marco, Sema3e, Wfdc10, Wwtr1, Pldb1, and Ifi205 microarray gene expression by quantitative PCR. Data are representative of 3 independent experiments.

donor-derived AMs. As a first step, we used fluorescent microscopy to demonstrate that host- and donor-derived AMs were located in the alveolar space with relatively equal ratios (Figure 4A). Because AMs of both origins were present in the alveolus, we instilled apoptotic cells, beads, or microbial particles via the intranasal route to examine phagocytic uptake within the same mouse. Whether the fluorescently labeled phagocytic targets were apoptotic cells, carboxylated beads, *E. coli* bioparticles, *S. aureus* bioparticles, or Zymosan A bioparticles, there appeared to be no selective phagocytic advantage for host- vs donor-derived AMs (Figure 4B-C). These findings were notable given the previously described roles of type A scavenger receptors, MARCO and scavenger receptor C-type lectin (collectin 12) in phagocytosis of microbial pathogens.[39,41] Because no difference in the clearance of *E. coli* bioparticles was observed between host- and donor-derived AMs, next we examined the production of inflammatory mediators from host- and donor-derived AMs containing *E. coli* (Figure 4C). To measure production of TNF-α and IL-1β by AMs in vivo, *E. coli* were instilled concomitantly with Brefeldin A. Four hours later, intracellular staining for proinflammatory cytokines was performed. Similar to phagocytosis, there was no detectable

difference for the production of TNFα and IL-1β by host- and donor-derived AMs (Figure 4C). Control quenching data illustrated that in vivo uptake of bioparticles by AMs were completely internalized after 2 hours of delivery compared with bioparticles given ex vivo to AMs on ice (Figure 4D). Overall, these data demonstrate that under homeostatic conditions and acute immune responses there appears to be no phagocytic or functional difference. However, it is unclear whether the persistence of donor-derived AM would affect the lungs long-term.

Relative gene expression in naïve mice for interstitial macrophages (postnatal-derived) and AMs (embyonic-derived)

Finally, we examined whether the genes selectively expressed by donor-derived AMs were expressed in pulmonary interstitial macrophages, known to derive from the same postnatal precursor cell, circulating blood monocytes.[47] The rationale for this experiment was to test the concept that there are some genes that are epigenetically conserved by macrophage donor-derived blood monocytes that cannot be altered by the environment. Accordingly, self-renewing host-derived AM
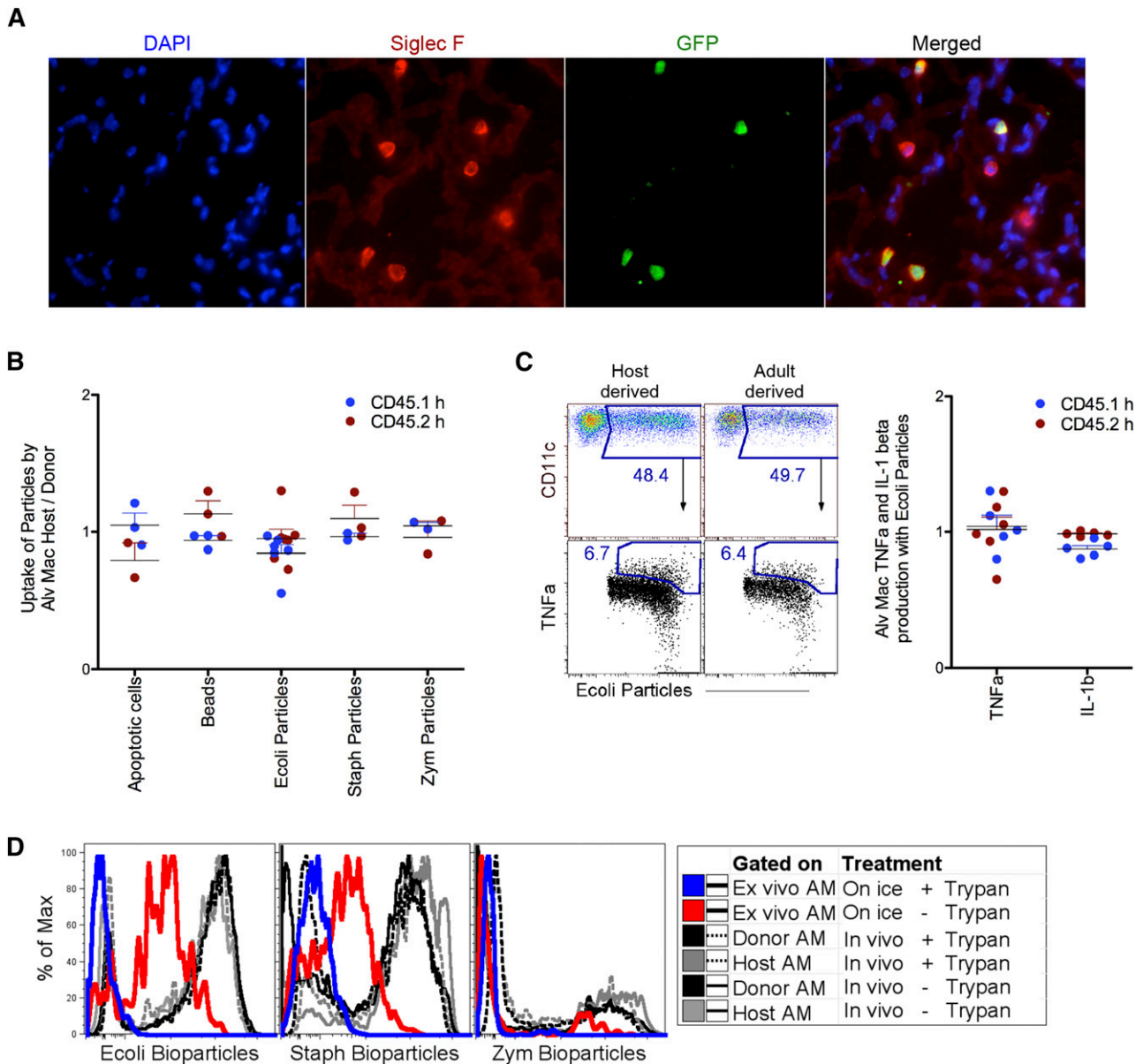
Figure 4. Functional analysis of host- and donor-derived AMs. (A) Microscopy staining around the alveolus for Siglec F[+] host-derived (GFP[−]) and donor-derived (GFP[+]) AMs was performed on lead shielded BM reconstituted mice 8-weeks post-CLL delivery. (B) Ratio analysis of host- over donor-derived AMs uptake for apoptotic cell, carboxylated beads, and bioparticles, 2 hours postintranasal delivery. (C) Flow cytometry gating strategy for 4B-4C (left) and ratio analysis of host- over donor-derived AMs for TNF-α and IL-1β production from AM with ingested *Escherichia coli* (right). Each dot represents one mouse. Blue dots represents analysis from set 1 and red dots represent analysis from set 2 (set 1 and set 2 as described in Figure 1A). (D) Two hours post-IN delivery of bioparticles, AMs were lavaged and quenched to exclude surface bound bioparticles. Black and gray lines are donor- and host-derived AM, dashed is quenched; solid line is unquenched. Control quenching was assessed with ex vivo AM given bioparticles on ice. Blue line is quenched; red line is unquenched. DAPI, 4,6 diamidino-2-phenylindole; GFP, green fluorescent protein.

and postnatal-derived interstitial macrophages were isolated from naïve mice and analyzed by microarray (Figure 5A).[11,48,49] Intriguingly, the data revealed that 8 of 10 genes that were identified in this study as being differentially expressed by donor-derived AMs compared with host-derived AMs were also selectively expressed by postnatal-derived interstitial macrophages: *Pyhin1*, *Retnla*, *Plbd1*, *C1qb*, *Slamf7*, *Ifi205*, *Akt3*, and *Mef2c* (Figure 5B). In comparison, 12 of 18 genes that were classified as being selectively expressed by host-derived AMs were not expressed by interstitial macrophages: *Marco*, *Sema3e*, *Wfdc10*, *Lphn3*, *Fam115a*, *Igf2bp2*, *Wwtr1*, *Erc2*, *Lepr*, *Prickle2*, *Meis1*, and *Lrig3* (Figure 5C). Overall, these data suggest that there are a few genes conserved by origin that cannot be altered by environment.

Discussion

From a global perspective, we found no substantial difference at either the transcriptional or functional level between host- and donor-derived AMs. This highlights that the environment strongly dictates and shapes the programming and function of AMs, independent of their original source. However, there were a small percentage of genes (~0.1% with a twofold or greater difference), such as *Marco*, whose expression was strongly associated with origin and not environment. In this regard, a recent epigenetic study revealed opened enhancer regions close to *Marco,* among other genes, that are present on all embryonic-derived
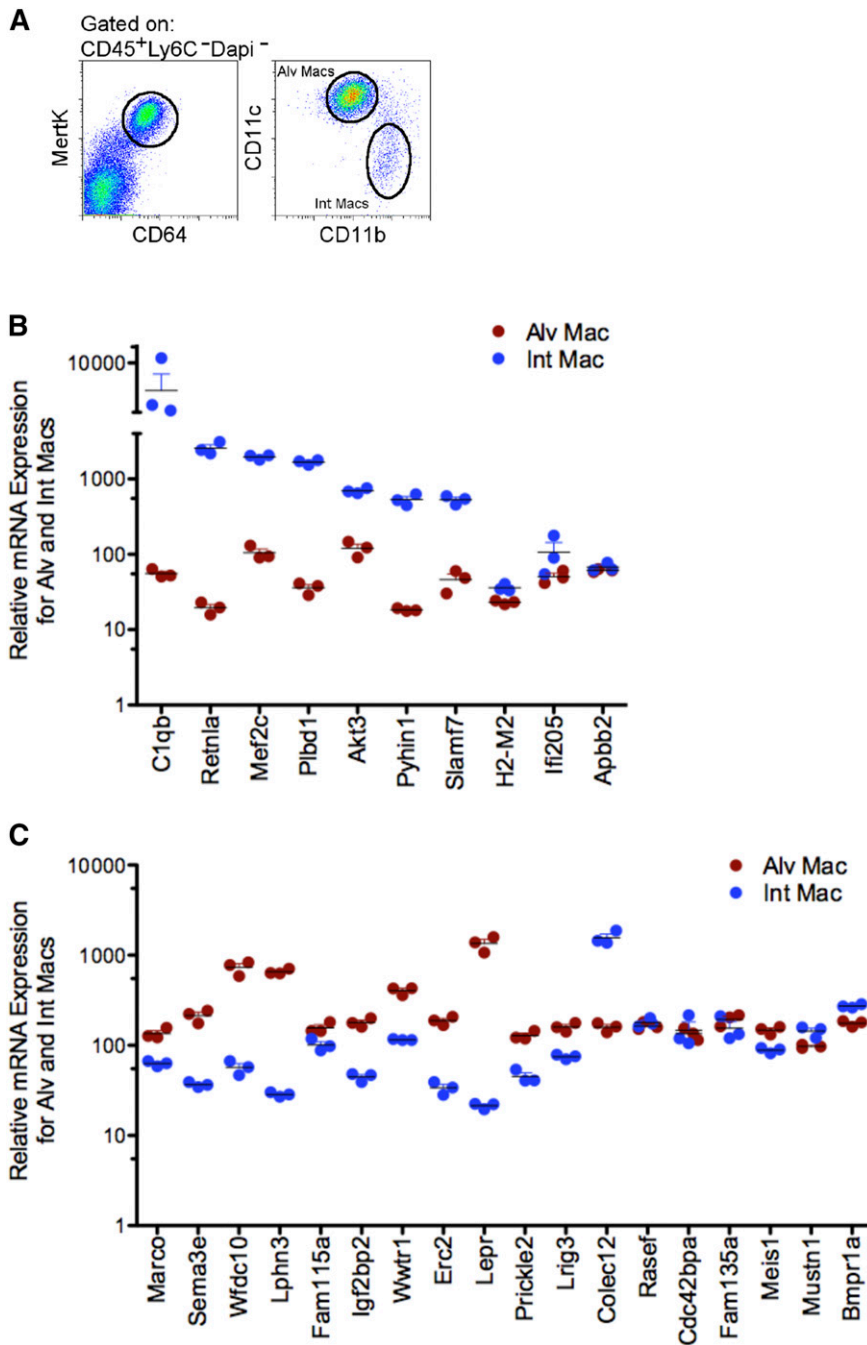
Figure 5. Selective gene analysis of alveolar and interstitial macrophages from naïve mice. (A) Identification CD45$^+$ (Lin$^-$: CD3$^-$ B220$^-$ NK1.1$^-$ Ly6C$^-$ Ly6G$^-$) CD64$^+$MertK$^+$, CD11c$^+$CD11b$^-$ alveolar and CD11c$^-$CD11b$^+$ interstitial macrophages. (B) Scatter plot of relative expression of messenger RNA (mRNA) for genes selectively expressed in favor of donor-derived AMs from alveolar (red) and interstitial (blue) macrophages isolated from naïve mice. Data shows triplicate sorts. (C) Scatter plot of relative expression of mRNA for genes selectively expressed in favor of host-derived AMs from alveolar (red) and interstitial (blue) macrophages isolated from naïve mice. Data illustrates triplicate sorts. Int Mac, interstitial macrophages.

macrophages, but not on postnatal-derived macrophages, such as intestinal macrophage and monocytes.[37] This would suggest that one could identify the origin of a macrophage based on the open or closed enhancer regions of *Marco*. However, it is important to note that not all opened enhancer regions identified[37] for embryonic-derived AMs were closed for donor-derived AMs. Indeed many genes that were selectively expressed by embryonic-derived AMs were also expressed by donor-derived AMs. Thus, environment will change the overall epigenetic landscape of a precursor cell regardless of its origin,[37] with the exception of a few genes that remain bound to its origin.

The implications of our findings may be profound because the genes linked to the donor-derived AM are genes that are expressed on postnatal-derived interstitial macrophages normally present within the tissue environment. Under homeostatic conditions, these postnatal-derived interstitial macrophages behave like reparative macrophages and are not functionally similar to resident embryonic-derived AMs. Thus, it is suggested that long-term, the cooperative relationship that normally exists between the AMs and interstitial macrophages may be tipped if both embryonic-derived AMs and postnatal-derived interstitial macrophages are derived from the same origin.

How closely these findings apply to humans is currently unknown. Overall our study complements the elegant epigenetic studies[37,50] while supporting an additional concept that there are a few genes conserved with origin that may not be altered by the environment. Our preliminary data from human studies may suggest that *Marco* can provide clues to a macrophages origin across species, because we observed high gene expression for *Marco* in human AMs compared with all other extravascular pulmonary myeloid cells and blood monocytes

(data not shown). In conclusion, although we did not observe any major functional differences with phagocytic and proinflammatory cytokine production between host- and donor-derived AMs in mice, it remains unknown whether the long-term presence of donor-derived AMs might alter the homeostatic balance that exists in the lungs when host-derived AMs are present.

Authorship

Contribution: C.V.J. and W.J.J. prepared the manuscript; R.G., A.N.D., and S.G. performed the experiments; C.V.J. and S.M.L. performed all bioinformatics analyses; and S.L.G., R.G., A.N.D., S.M.L., M.P., S.M.A., D.L.B., W.J., and C.V.J. provided intellectual input, designed experiments, provided critical feedback, and discussed results.

Conflict-of-interest disclosure: The authors declare no competing financial interests.

Correspondence: Claudia Jakubzick, National Jewish Health, Department of Pediatrics and Immunology, 1400 Jackson St, Denver, CO 80206; e-mail: jakubzickc@njhealth.org.

References

1. MacLean JA, Xia W, Pinto CE, Zhao L, Liu HW, Kradin RL. Sequestration of inhaled particulate antigens by lung phagocytes. A mechanism for the effective inhibition of pulmonary cell-mediated immunity. *Am J Pathol.* 1996;148(2):657-666.

2. Thepen T, Van Rooijen N, Kraal G. Alveolar macrophage elimination in vivo is associated with an increase in pulmonary immune response in mice. *J Exp Med.* 1989;170(2):499-509.

3. Thepen T, Kraal G, Holt PG. The role of alveolar macrophages in regulation of lung inflammation. *Ann N Y Acad Sci.* 1994;725:200-206.

4. Guilliams M, Lambrecht BN, Hammad H. Division of labor between lung dendritic cells and macrophages in the defense against pulmonary infections. *Mucosal Immunol.* 2013;6(3):464-473.

5. Gautier EL, Shay T, Miller J, et al; Immunological Genome Consortium. Gene-expression profiles and transcriptional regulatory pathways that underlie the identity and diversity of mouse tissue macrophages. *Nat Immunol.* 2012;13(11):1118-1128.

6. Zhang X, Goncalves R, Mosser DM. The isolation and characterization of murine macrophages. *Curr Protoc Immunol.* 2008;11.

7. Sawyer RT. The significance of local resident pulmonary alveolar macrophage proliferation to population renewal. *J Leukoc Biol.* 1986;39(1):77-87.

8. Coggle JE, Tarling JD. The proliferation kinetics of pulmonary alveolar macrophages. *J Leukoc Biol.* 1984;35(3):317-327.

9. Guilliams M, De Kleer I, Henri S, et al. Alveolar macrophages develop from fetal monocytes that differentiate into long-lived cells in the first week of life via GM-CSF. *J Exp Med.* 2013;210(10):1977-1992.

10. Hashimoto D, Chow A, Noizat C, et al. Tissue-resident macrophages self-maintain locally throughout adult life with minimal contribution from circulating monocytes. *Immunity.* 2013;38(4):792-804.

11. Jakubzick C, Gautier EL, Gibbings SL, et al. Minimal differentiation of classical monocytes as they survey steady-state tissues and transport antigen to lymph nodes. *Immunity.* 2013;39(3):599-610.

12. Schulz C, Gomez Perdiguero E, Chorro L, et al. A lineage of myeloid cells independent of Myb and hematopoietic stem cells. *Science.* 2012;336(6077):86-90.

13. Yona S, Kim KW, Wolf Y, et al. Fate mapping reveals origins and dynamics of monocytes and tissue macrophages under homeostasis. *Immunity.* 2013;38(1):79-91.

14. Gomez Perdiguero E, Klapproth K, Schulz C, et al. Tissue-resident macrophages originate from yolk-sac-derived erythro-myeloid progenitors. *Nature.* 2015;518(7540):547-551.

15. Epelman S, Lavine KJ, Randolph GJ. Origin and functions of tissue macrophages. *Immunity.* 2014;41(1):21-35.

16. Janssen WJ, Barthel L, Muldrow A, et al. Fas determines differential fates of resident and recruited macrophages during resolution of acute lung injury. *Am J Respir Crit Care Med.* 2011;184(5):547-560.

17. Ginhoux F, Tacke F, Angeli V, et al. Langerhans cells arise from monocytes in vivo. *Nat Immunol.* 2006;7(3):265-273.

18. Blériot C, Dupuis T, Jouvion G, Eberl G, Disson O, Lecuit M. Liver-resident macrophage necroptosis orchestrates type 1 microbicidal inflammation and type-2-mediated tissue repair during bacterial infection. *Immunity.* 2015;42(1):145-158.

19. Landsman L, Varol C, Jung S. Distinct differentiation potential of blood monocyte subsets in the lung. *J Immunol.* 2007;178(4):2000-2007.

20. Jakubzick C, Tacke F, Llodra J, van Rooijen N, Randolph GJ. Modulation of dendritic cell trafficking to and from the airways. *J Immunol.* 2006;176(6):3578-3584.

21. Careau E, Bissonnette EY. Adoptive transfer of alveolar macrophages abrogates bronchial hyperresponsiveness. *Am J Respir Cell Mol Biol.* 2004;31(1):22-27.

22. Berg JT, Lee ST, Thepen T, Lee CY, Tsan MF. Depletion of alveolar macrophages by liposome-encapsulated dichloromethylene diphosphonate. *J Appl Physiol (1985).* 1993;74(6):2812-2819.

23. Matute-Bello G, Lee JS, Frevert CW, et al. Optimal timing to repopulation of resident alveolar macrophages with donor cells following total body irradiation and bone marrow transplantation in mice. *J Immunol Methods.* 2004;292(1-2):25-34.

24. Nakata K, Gotoh H, Watanabe J, et al. Augmented proliferation of human alveolar macrophages after allogeneic bone marrow transplantation. *Blood.* 1999;93(2):667-673.

25. Wickenhauser C, Thiele J, Pérez F, et al. Mixed chimerism of the resident macrophage population after allogeneic bone marrow transplantation for chronic myeloid leukemia. *Transplantation.* 2002;73(1):104-111.

26. Janssen WJ, Muldrow A, Kearns MT, Barthel L, Henson PM. Development and characterization of a lung-protective method of bone marrow transplantation in the mouse. *J Immunol Methods.* 2010;357(1-2):1-9.

27. Gautier EL, Shay T, Miller J, et al. Gene-expression profiles and transcriptional regulatory pathways that underlie the identity and diversity of mouse tissue macrophages. *Nat Immunol* 2012;13(11):1118-1128.

28. Jakubzick C, Helft J, Kaplan TJ, Randolph GJ. Optimization of methods to study pulmonary dendritic cell migration reveals distinct capacities of DC subsets to acquire soluble vs particulate antigen. *J Immunol Methods.* 2008;337(2):121-131.

29. Hunter L, Taylor RC, Leach SM, Simon R. GEST: a gene expression search tool based on a novel Bayesian similarity metric. *Bioinformatics.* 2001;17(Suppl 1):S115-S122.

30. Smyth GK. Linear models and empirical bayes methods for assessing differential expression in microarray experiments. *Stat Appl Genet Mol Biol.* 2004;3:Article3.

31. Gentleman RC, Carey VJ, Bates DM, et al. Bioconductor: open software development for computational biology and bioinformatics. *Genome Biol.* 2004;5(10):R80.

32. Jakubzick C, Tacke F, Ginhoux F, et al. Blood monocyte subsets differentially give rise to CD103+ and CD103- pulmonary dendritic cell populations. *J Immunol.* 2008;180(5):3019-3027.

33. Robays LJ, Maes T, Lebecque S, et al. Chemokine receptor CCR2 but not CCR5 or CCR6 mediates the increase in pulmonary dendritic cells during allergic airway inflammation. *J Immunol.* 2007;178(8):5305-5311.

34. Misharin AV, Morales-Nebreda L, Mutlu GM, Budinger GR, Perlman H. Flow cytometric analysis of macrophages and dendritic cell subsets in the mouse lung. *Am J Respir Cell Mol Biol.* 2013;49(4):503-510.

35. Tateno H, Crocker PR, Paulson JC. Mouse Siglec-F and human Siglec-8 are functionally convergent paralogs that are selectively expressed on eosinophils and recognize 6′-sulfo-sialyl Lewis X as a preferred glycan ligand. *Glycobiology.* 2005;15(11):1125-1135.

36. Pan J, Li S, Chi P, Xu Z, Lu X, Huang Y. Lentivirus-mediated RNA interference targeting WWTR1 in human colorectal cancer cells inhibits cell proliferation in vitro and tumor growth in vivo. *Oncol Rep.* 2012;28(1):179-185.

37. Lavin Y, Winter D, Blecher-Gonen R, et al. Tissue-resident macrophage enhancer landscapes are shaped by the local microenvironment. *Cell.* 2014;159(6):1312-1326.

38. Benard EL, Roobol SJ, Spaink HP, Meijer AH. Phagocytosis of mycobacteria by zebrafish macrophages is dependent on the scavenger receptor Marco, a key control factor of pro-inflammatory signalling. *Dev Comp Immunol.* 2014;47(2):223-233.

39. Józefowski S. [The role of the class A scavenger receptors, SR-A and MARCO, in the immune system. Part 2. Contribution to recognition and phagocytosis of pathogens as well as induction of immune response]. *Postepy Hig Med Dosw (Online).* 2012;66:120-131.

40. Arredouani M, Yang Z, Ning Y, et al. The scavenger receptor MARCO is required for lung defense against pneumococcal pneumonia and inhaled particles. *J Exp Med.* 2004;200(2):267-272.

41. Jang S, Ohtani K, Fukuoh A, et al. Scavenger receptor collectin placenta 1 (CL-P1) predominantly mediates zymosan phagocytosis by human vascular endothelial cells. *J Biol Chem.* 2009;284(6):3956-3965.

42. Ohtani K, Suzuki Y, Eda S, et al. The membrane-type collectin CL-P1 is a scavenger receptor on vascular endothelial cells. *J Biol Chem.* 2001; 276(47):44222-44228.

43. Steffen A, Koestler SA, Rottner K. Requirements for and consequences of Rac-dependent protrusion. *Eur J Cell Biol.* 2014;93(5-6):184-193.

44. Haque A, Koide N, Odkhuu E, et al. Mouse pyrin and HIN domain family member 1 (pyhin1) protein positively regulates LPS-induced IFN-β and NO production in macrophages. *Innate Immun.* 2014; 20(1):40-48.

45. Schattgen SA, Fitzgerald KA. The PYHIN protein family as mediators of host defenses. *Immunol Rev.* 2011;243(1):109-118.

46. Kim JR, Horton NC, Mathew SO, Mathew PA. CS1 (SLAMF7) inhibits production of proinflammatory cytokines by activated monocytes. *Inflamm Res.* 2013;62(8):765-772.

47. Plantinga M, Guilliams M, Vanheerswynghels M, et al. Conventional and monocyte-derived CD11b(+) dendritic cells initiate and maintain T helper 2 cell-mediated immunity to house dust mite allergen. *Immunity.* 2013;38(2):322-335.

48. Scott CL, Henri S, Guilliams M. Mononuclear phagocytes of the intestine, the skin, and the lung. *Immunol Rev.* 2014;262(1):9-24.

49. Guilliams M, Ginhoux F, Jakubzick C, et al. Dendritic cells, monocytes and macrophages: a unified nomenclature based on ontogeny. *Nat Rev Immunol.* 2014;14(8):571-578.

50. Gosselin D, Link VM, Romanoski CE, et al. Environment drives selection and function of enhancers controlling tissue-specific macrophage identities. *Cell.* 2014;159(6):1327-1340.